Ocean Systems Engineering, *Vol. 13, No. 1 (2023) 43-55*
https://doi.org/10.12989/ose.2023.13.1.043

Stress concentration factors in tubular T-joints stiffened with external ring under axial load

Hossein Nassiraei*[1] and Pooya Rezadoost[2b]

[1]*Department of Civil Engineering, Faculty of Engineering, University of Guilan, Guilan, Iran*
[2]*Faculty of Civil Engineering, K.N. Toosi University of Technology, Tehran, Iran*

(Received January 3, 2023, Revised March 12, 2023, Accepted March 14, 2023)

Abstract. In this study, the SCFs in tubular T-joints stiffened with external ring under axial load are studied and discussed. After verification of the present numerical model with the results of several available experimental tests, 156 FE models were generated and analyzed to parametrically evaluate the effect of the joint geometry and the ring geometry on the SCFs. Results indicated that the SCF of the stiffened T-joints at crown point can be down to 24% of the SCF of the corresponding un-reinforced joint at the same point. Also, the effect of the ring on the SCF at saddle point is more remarkable than the effect of the ring on the SCF at crown point. Moreover, against un-reinforced joints under axial load, the SCF at saddle point of the stiffened joint is smaller than the SCF at crown point of that stiffened joint. The ring results in the redistribution of stresses in the ring and metal substrate. Also, the effect of the ring thickness on the decrease of the SCFs is slight and can be ignored. In final step, the geometric parameters affecting the SCFs of the stiffened T-joints are analyzed by multiple nonlinear regression analyses. An accurate formula is proposed for determining the SCFs.

Keywords: axial load; offshore structures; parametric equation; ring; SCF; T-joints

1. Introduction

Circular hollow section (CHS) members are generally applied as the main components in offshore tubular structures such as jacket-type platforms. The CHS members are connected to form a tubular joint. The intersection between the tubular joints is always prone to high-stress concentration because of its geometric complexity and welding defects (Mohamed *et al*. 2022). Under the operating conditions and climatic hazards on the site of the offshore structures, such as cyclic loads induced by wind and sea waves, fatigue failure becomes the main cause of the collapse in the absence of accidents (Xu *et al*. 2022). To evaluate the fatigue life of tubular joints, the conventional method of combining hot spot stress (HSS) with a suitable S–N curve is widely applied. Generally, the hot spot stress (HSS) can be calculated by multiplying the SCF by the normal stress in the brace. Afterward, precise prediction of SCF is of primary importance for assessing the fatigue life of tubular joints (Pan *et al*. 2022).

Several works are conducted on the SCF of un-reinforced tubular T-, Y-, and X-joints. For

*Corresponding author, Assistant Professor, E-mail: h.nassiraei@guilan.ac.ir
[a]Ph.D. Student, E-mail: p.rezadoost@email.kntu.ac.ir

http://www.techno-press.org/?journal=ose&subpage=7 ISSN: 2093-6702 (Print), 2093-677X (Online)

example, JISSP (1986), Kratzer (1981), Swensson and Yura (1986), United Kingdom offshore steels research project (1980), and Wordsworth (1979) carried out some experimental tests on this matter. Also, Chang and Dover (1999) proposed some empirical equations for determining the SCF in un-reinforced tubular T-joints. The stress distribution in un-reinforced T-joints was studied by Shao (2007). The effect of the combined axial, bending, and dynamic loading on the SCFs in tubular T-joints was assessed by N'Diaye *et al*. (2009). The results showed that the increase of dynamic SCFs leads to the appearance of fatigue damage, due to cracking at the hot spot stress (HSS) point. The efficacy of the weld geometries on the SCFs investigated by Hectors and Waele (2021). The results indicated that the geometry of the weld has a notable effect on the maximum SCF. Gho *et al*. (2006) proposed some formulas for calculating the SCF in overlapped thin-walled CHS joints under axial load. Liu *et al*. (2002) investigated the stress influence matrix on hot spot stress analysis. N'Diaye *et al*. (2009) proved that the tubular joints should be stiffened to ensure sufficient fatigue life for offshore structures. Also, several works are carried out on stiffened tubular joints. These stiffening methods include internal rings (Pan *et al*. 2022, Ahmadi *et al*. 2022), fiber reinforced polymer (Nassiraei and Rezadoost 2020, Nassiraei and Rezadoost 2022, Hosseini *et al*. 2020), collar plates (Cai and Shao 2011, Nassiraei 2020), Doubler plates (Fung *et al*. 2002, Nassiraei 2022, Soh and Soh 1995), grout (Shen and Choo 2012), concrete (Musa *et al*. 2018, Tong *et al*. 2019, Xu *et al*. 2015), rack/rib (Myers *et al*. 2001), and ring (Zhu *et al*. 2017).

It can be concluded that, so far, no experimental/numerical/theoretical work is conducted on the SCF in T-joints with the external ring under axial load (Fig. 1). Consequently, this is the first available study on this problem. Investigation on the effect of the joint geometry (τ, γ, and β) and ring geometry (τ_{ring} and β_{ring}) on the SCF is innovation of this paper. Also, proposing a new formula for determining the SCF in T-joints with outer ring under axial load is innovation of the present study. On the other hand, the ring can significantly decrease the SCFs. Moreover, it can be used for reinforcing tubular joint in the structures during both design and operation. However, it should be noted that under the water it is costly to implement such a retrofit ring.

In this work, in the first step, the details of the FE modeling are introduced. After that, the present numerical model is validated by the experimental results reported by JISSP (1986), Kratzer (1981), Swensson and Yura (1986), United Kingdom offshore steels research project (1980), Wordsworth (1979), Zhu *et al*. (2017), and Zhao *et al*. (2020). In the following step, in the parametric study, 156 FE models are produced (Fig. 1). In the next step, using the generated FE models, the effect of the joint geometry (τ, γ, and β) and ring geometry (τ_{ring} and β_{ring}) are investigated on the SCFs. In the final step, for the determining the SCFs in the stiffened T-joints at crown and saddle locations, a parametric formula is derived. Applicability of the proposed equation is validated based on the experimental results and the UK Department of Energy (1980) criteria.

2. FE modeling

The weld profile is designed based on the recommendations given by the American Welding Society (A.W.S) (2015). All FE models are modeled using the SOLID186 element. The element has 20 nodes having three degrees of freedom per node. The meshed joint is shown in Fig. 2.

The element size near the weld is very small. Farther from the weld, a greater element size is applied together with tetrahedral elements, to obtain an optimized mesh. Also, only one-fourth of the T-joints were created, because of the symmetry in the geometry and loading conditions. In addition, the displacements and rotations of both chord ends were fixed.

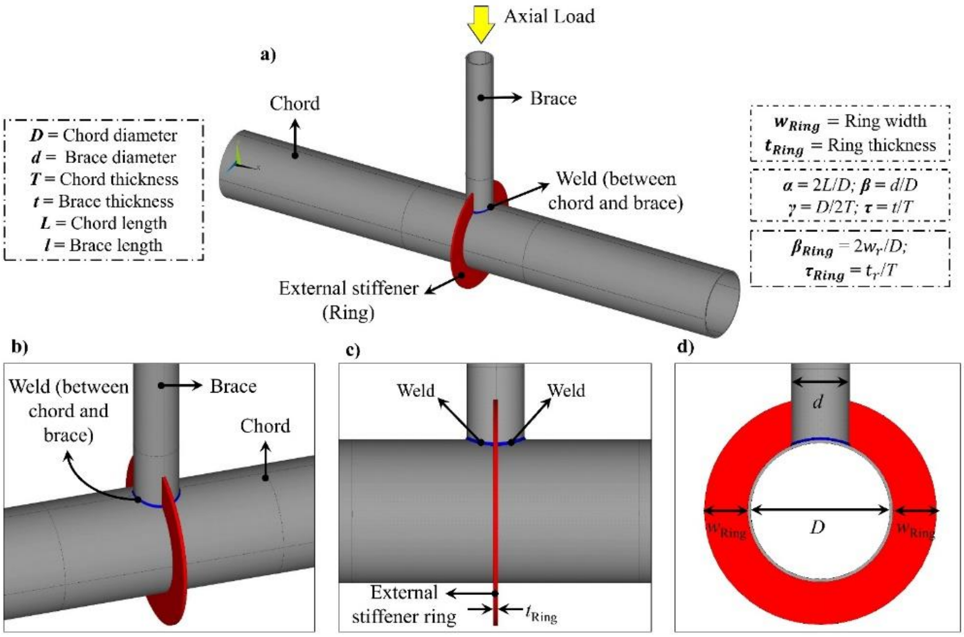

Fig. 1 Geometrical notation for T-joint reinforced with ring

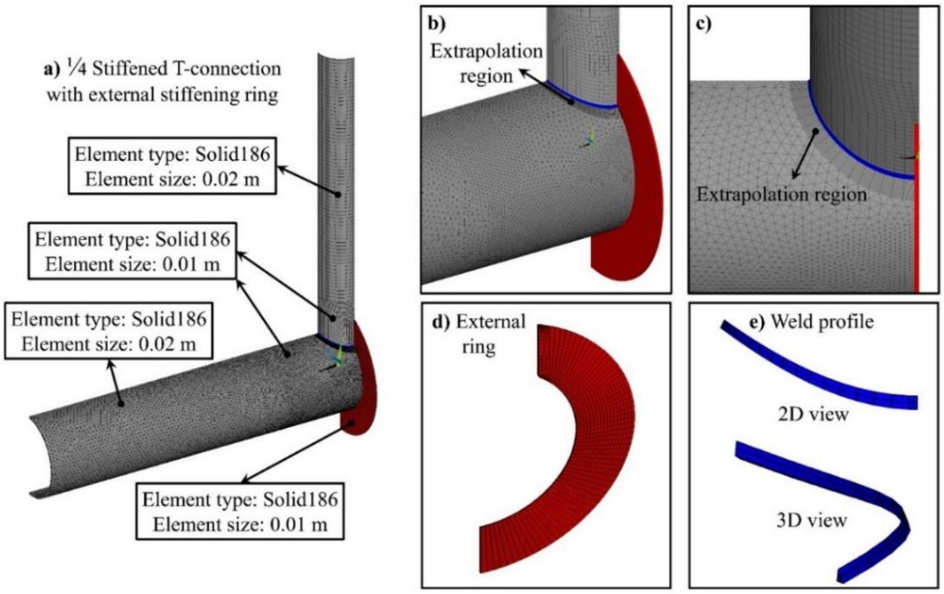

Fig. 2 The generated mesh and extrapolation zone

To obtain the SCFs, a linearly static analysis is appropriate (Bao *et al*. 2022, Nassiraei and Rezadoost 2021a). The “hot spot” is defined as the location along the weld toe, where the

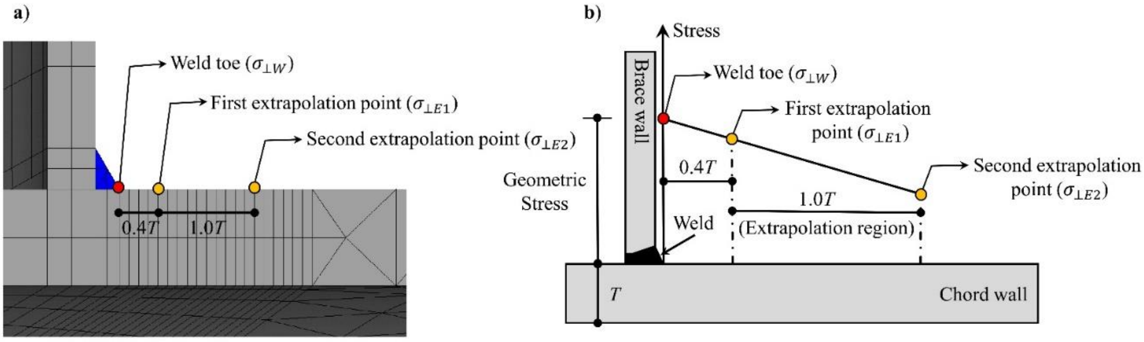

Fig. 3 SCF calculation. (a) the enlarged extrapolation region with details and (b) the extrapolation procedure

extrapolated stress has a peak value (Jiang *et al*. 2018). Also, the stress component perpendicular to the weld toe is chosen to carry out the line extrapolation for determining the hot spot stress (HSS), based on, International Institute of Welding (IIW) (2008), Comité International pour le Développement et l´Étude de la Construction Tubulaire (CIDECT) (2000), and American Petroleum Institute (API) (2015). The region from which the stresses have to be extrapolated, the so-called "extrapolation region" (CIDECT 2000), is shown in Fig. 3. The HSS along joint crossing (Fig. 3) can be determined as expressed in Eq. (1).

$$\sigma_{\perp \mathrm{W}} = 1.4\sigma_{\perp \mathrm{E1}} - 0.4\sigma_{\perp \mathrm{E2}} ? \tag{1}$$

Where the $\sigma_{\perp E1}$ and $\sigma_{\perp E2}$ are the stresses at a distance of Δ_1 and Δ_2 from the weld toe in the direction perpendicular to the weld toe, correspondingly. Δ_1 and Δ_2 are equal to 0.4T and 1.4T, respectively. They are indicated in Fig. 3. The stress at an extrapolation location can be calculated by Eq. (2). In Eq. (2), $\sigma_{\perp N1}$ and $\sigma_{\perp N2}$ are the nodal stresses near the extrapolation location along the vertical direction to the weld toe; δ_1 and δ_2 are the intervals between the nodes and the weld toe. The SCF value can be determined by Eq. (3). In this equation, σ_n is the nominal stress. For a joint under axial load (F), σ_n can be obtained by Eq. (4). The r and t are the radius and thickness of the brace member. This method is performed for all 156 FE specimens.

$$\sigma_{\perp \mathrm{E}} = \frac{\sigma_{\perp N1} - \sigma_{\perp N2}}{\delta_1 - \delta_2}(\Delta_i - \delta_2) + \sigma_{\perp N2} \tag{2}$$

$$SCF = \sigma_{\perp W} / \sigma_n \tag{3}$$

$$\sigma_n = \frac{F}{\pi(r^2 - (r-t)^2)} \tag{4}$$

3. Validation of the numerical model

The numerical procedure should be validated with the experimental data. There is no available experimental/FE/theoretical result in the past works on the SCF in joints with ring. Therefore, the

Table 1 Geometrical parameters of experimental tests

Specimen	D (mm)	α	β	γ	τ	θ (°)	Joint & Load type	Ref.
S1	508	6.20	0.80	20.3	0.99	90	T, Axial, Un-stiffened	JISSP (1986)
S2	328.3	12.00	0.67	25.9	1.00	90	T, Axial, Un-stiffened	Sadat Hosseini *et al.* (2020)
S3	152	13.50	0.50	12.0	0.52	90	T, Axial, Un-stiffened	UKOSRP (1980)
S4	150	16.00	0.50	24.0	1.00	45	Y, Axial, Un-stiffened	Wordsworth (1979)
S5	299.8	12.05	0.73	18.62	1.00	90	X, Compression, Stiffened with external ring	Zhu *et al.* (2017)
S6	300	12.00	0.51	18.67	1.02	90	X, Tension, Stiffened with external ring	Zhu *et al.* (2020)

Table 2 Material properties of experimental tests

Specimen	Chord*			Brace*			External*		
	E (GPa)	Fy (MPa)	Fu (MPa)	E (GPa)	Fy (MPa)	Fu (MPa)	E (GPa)	Fy (MPa)	Fu (MPa)
S1, S3, S4	207	-	-	207	-	-	-	-	-
S2	200	385	510	200	383	498	-	-	-
S5	194	325	466	200	321	489	209	315	436
S6	198	291	-	208	357	-	209	315	-

* In all connections, υ is equal to 0.3

Table 3 Comparison between numerical and experimental results

Specimen	Position	Experimental Test	FE	Exp/FE
S1	Crown	5.40	4.87	1.11
	Saddle	11.40	10.93	1.04
S2	Crown	4.97	5.34	0.93
	Saddle	26.15	25.92	1.01
S3	Saddle	5.90	5.89	1.00
S4	Saddle	7.50	7.60	0.99
Mean error between experimental and numerical results				0.04

presented experimental tests in Tables 1 and 2 are used. The geometrical details of the tests are listed in Table 1. In addition, the material properties of the members are listed in Table 2. The numerical models were carried out and analyzed in ANSYS. Specimens S1 to S4 verify the accuracy of the SCF calculation at the crown and saddle position and specimens S5 and S6 verify the accuracy of the modeling and analysis of reinforced joints.

Table 3 lists the SCFs at crown and saddle locations of the un-reinforced tubular joints. It can be seen that in all 6 locations, the present FE results and experimental data are close. The maximum

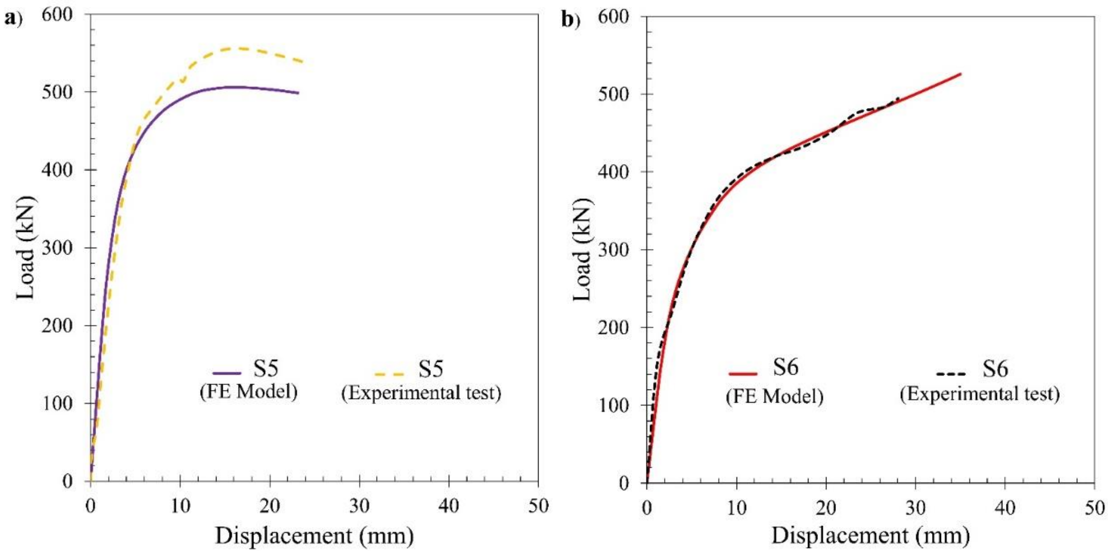

Fig. 4 The comparison between the experimental data and numerical results

and average difference between the SCF of the experimental data and numerical results are equal to 11% and 4%, respectively. Figs. 4(a) and 4(b) present the load-displacement curves for two tubular joints with the ring under axial load. It can be seen that the FE model can well predict the behavior of the tubular joints with the ring. Hence, it can be concluded that the present 3-D FE model is capable of simulating the SCFs of T-joints with and without the ring under axial load with enough accuracy.

4. Parametric assessment program

4.1 General

156 FE models were created, using the commercial ANSYS software, to assess the efficacy of the ring thickness (τ_{ring}), ring width (β_{ring}), and joint geometry (τ, β, and γ) on the SCFs at both crown and saddle locations in the T-joints without and with the ring under axial load. The weld material is similar to the material of the members, based on the recommendations of previous research. The numerical models have been considered with Young's modulus (E) of 207 GPa and Poisson's ratio (v) of 0.3.

4.2 Effect of τ

Figs. 5(a)-5(f) indicate the change of the SCFs at crown and saddle locations, because of the variations in the value of τ and the ring geometry (β_{ring} and τ_{ring}). Due to this aim, 52 FE specimens were created and analyzed with four different values of the τ (τ = 0.4, 0.6, 0.8, and 1.0), three diverse values of β_{ring} (β_{ring} = 0.2, 0.6, and 1.0), and four various values of the τ_{ring} (τ_{ring} = 0.5, 1.0, 1.5, and 2.0). It should be noted that Yang *et al*. (2018) investigated the tubular X-joints reinforced with the

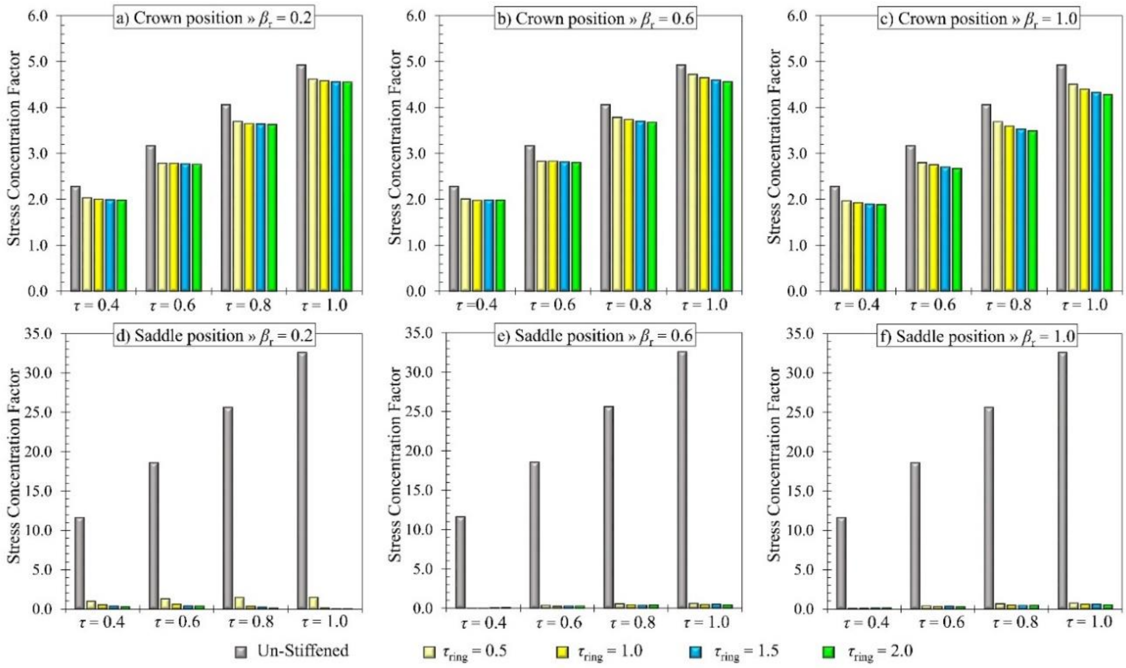

Fig. 5 Effect of the τ on the SCFs (γ = 28 and β = 0.5)

external ring. They investigated up to τ_{ring} = 1.5. Melek *et al*. (2020) studied the effect of the external ring on the ultimate strength of T-joints. They investigated up to τ_{ring} = 1.75. Nassiraei and Rezadoost (2021b) investigated the effect of the external ring on the tubular joints. They used the ring up to τ_{ring} = 2. Hence, this range (τ_{ring} = 0.5, 1.0, 1.5, and 2.0) is used for investigating the τ_{ring}. In the following step, the results are compared with their un-reinforced joint results. Fig. 5 shows that in all joints reinforced with the ring, the increase of the τ, in constant chord thickness, causes the strong raise of the SCFs. To illustrate, in the joints with γ = 28, β = 0.5, τ_{ring} = 2, and β_{ring} = 0.2 (Fig. 5(a)), the SCF for the joints with τ = 0.6 and 1.0 are equal to 2.77 and 4.56, respectively. Moreover, it can be observed that the use of the ring can show the remarkable decrement in the SCFs. Because, the ring enhances the stiffens of the joint intersection against ovalization and local bending of the chord. Also, the increase of each the ring thickness or the ring width can lead to the decrease in the SCFs. However, the effect of the ring width on the SCFs is slight. It can be seen that the SCFs in the reinforced joints at saddle positions (Figs. 5(d)-5(f)) are smaller than 1.5. On the other hand, API (2015) recommended that for all welded tubular joints under axial loading, a minimum SCF of 1.5 should be applied. Consequently, the SCFs at the saddle points should be considered equal to 1.5.

4.3 Effect of γ

In this section, the effects of the γ on the SCFs are discussed. A set of 52 numerical models are generated with four various values of the γ, four different values of the τ_{ring}, and three varied values of the β_{ring}. After that, the results are compared with the results of corresponding un-reinforced joints.

Figs. 6(a)-6(f) indicates that the use of ring leads to the decrease of the SCFs. Because, the use of the ring leads to redistribution of stresses in the ring and metal substrate. This phenomenon is

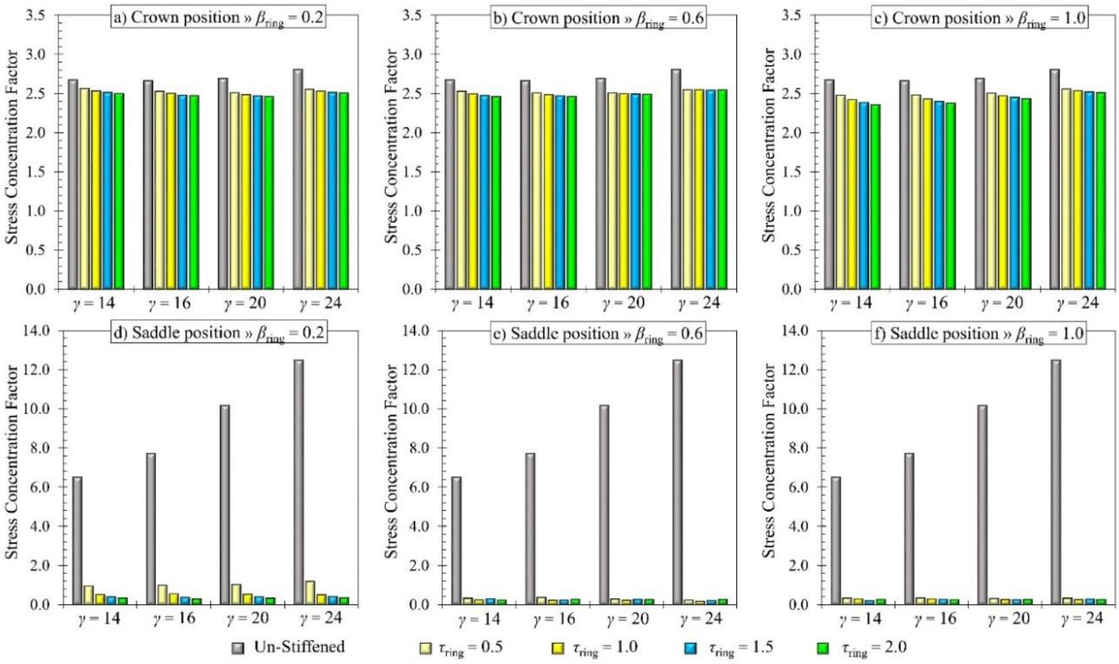

Fig. 6 Effect of the γ on the SCFs (β = 0.6 and τ = 0.5)

more notable at the saddle point. Because the ring is placed in this location. For example, in the joints with β = 0.6, τ = 0.5, γ = 16 at crown point (Fig. 6(b)), the SCFs for the reinforced joint (β_{ring} = 1.0, τ_{ring} = 2.0) and un-reinforced joint are equal to 2.46 and 2.58, respectively. But, the SCFs in the same joints at saddle location are equal to 0.27 and 12.49, respectively. Also, it should be noted that in un-reinforced T-joints under axial load, saddle point is critical. Hence, the ring is a valuable technique for decreasing in the SCFs and enhancing the fatigue life in the T-joints. In addition, the results illustrate that the effect of the γ on the SCFs is slight. Figs. 6(d)-7(f) show that the SCFs in the reinforced joints at saddle positions are smaller than 1.5. Hence, according to API (2015), the SCFs at the saddle points should be considered equal to 1.5.

4.4 Effect of β

Six charts in Fig. 7 present the SCFs in the un-reinforced and reinforced joins at crown and saddle locations. For this aim, 52 FE models are generated and analyzed with four various values of the β (β = 0.2, 0.4, 0.6, and 0.8, three different values of the ring width factor (β_{ring} = 0.2, 0.6, and 1.0), and four various values of the ring thickness factor (τ_{ring} = 0.5, 1.0, 1.6, and 2.0). In the following stage, the results are compared with their un-reinforced joint results.

The results indicate that the utilization of the ring can lead to the decrease of the SCFs. The decrement is very more remarkable at the saddle point, lead to than the crown point. Because, the ring is placed at the saddle location. As shown in Fig. 7, in the un-reinforced joints, the SCFs at saddle locations are remarkably bigger than the corresponding SCFs at crown points. On the contrary, in the reinforced joints, the SCFs as saddle points are significantly smaller than the corresponding SCFs at crown locations. The results show that the effect of the ring the thickness on the SCFs is

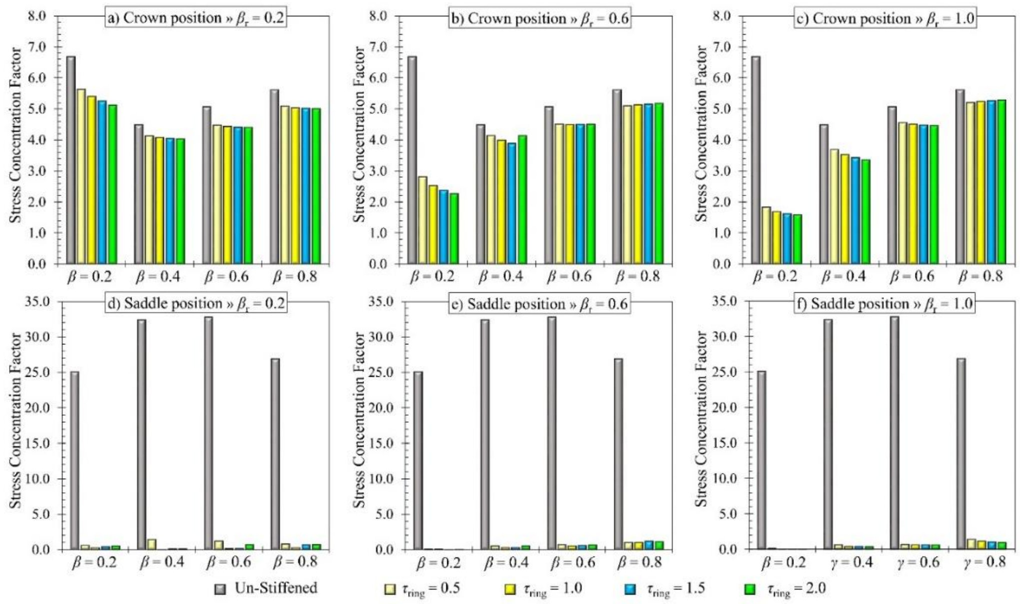

Fig. 7 Effect of the β on the SCFs (γ = 32 and τ = 0.9)

more remarkable than the effect of the ring width on the SCFs. From Figs. 7(d)-7(f), the SCFs in the reinforced joints at saddle positions should be considered equal to 1.5. Because, API (2015) suggested that for all tubular joints, a minimum SCF of 1.5 should be used.

5. Deriving formula

So far, no equation is existing for determining the SCFs in any joints reinforced with ring. Hence, a parametric equation is proposed for determining the SCFs in the T-joints with ring under axial load. To this aim, the statistical evaluation of the SCFs has been done using SPSS V21, and the following formula is established.

$$SCF_{crown} = 50.52\beta^{0.063}\beta_{ring}^{1.317}\tau^{0.928}\tau_{ring}^{-0.003}-49\tau^{0.933}\beta_{ring}^{1.306}+3.6\,\tau^{0.955}\gamma^{0.106}\ ;\ R^2 = 0.945 \quad (5)$$

$$SCF_{saddle} = 1.5 \quad (6)$$

In Eq. (5), the SCF_{crown} shows the SCF in the reinforced joint at the crown location. In Eq. (6), the SCF_{saddle} presents the SCF in the reinforced joint at the saddle location. R^2 indicates the factor of determination. Its value for the derived formula is regarded to be acceptable. The following ranges of geometric parameters are valid for the application of Eq. (7).

$$0.2 \le \beta_{ring} \le 1.0,$$
$$0.5 \le \tau_{ring} \le 2,$$
$$0.4 \le \tau \le 1.0,$$
$$12 \le \gamma \le 28,$$
$$0.2 \le \beta \le 0.8 \quad (7)$$

Table 4 Evaluation of the formula based on the UK DoE (1980) criteria

Proposed formula	%*P*/M** < 0.8	%*P/M* > 1.5
Eq. (5)	1.4% < 5% OK.	0.0% < 50% OK.

**P* is the SCF value calculated by the proposed equation and *M* is the SCF value obtained from the FE analysis

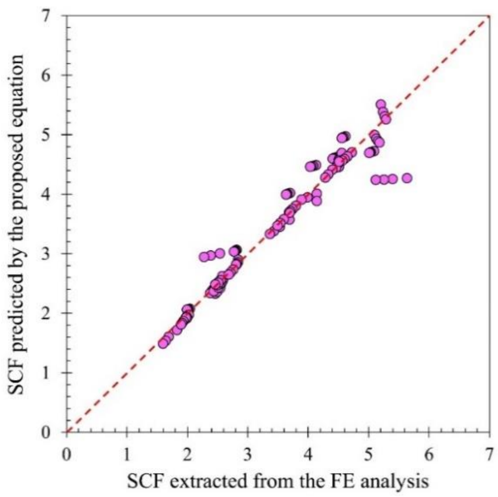

Fig. 8 Comparison of the SCF ratios predicted by the equation with the SCF ratios extracted from FE analysis

The UK Department of Energy (1980) suggests the below assessment criteria. In the assessment, P means the predicted value. M means the measured value.

- If [P/M < 0.8] ≤ 5%; and [P/M < 1.0] ≤ 25%, the formula is accepted. If moreover, [P/M > 1.5] ≥ 50%, the formula is taken as generally circumspect.
- If 5% < [P/M < 0.8] ≤ 7.5%, and/or 25% < [P/M < 1.0] ≤ 30%, the formula is taken as borderline. Consequently, more assessment should be conducted.
- Otherwise, the established equation cannot be approved. Since, it is too optimistic.

Based on the suggestions of Bomel Consulting Engineers (1994), P/R < 1.0 can be eliminated in the assessment. Evaluating Eq. (5) according to the UK DoE (1980) standard is tabulated in Table 4. As shown, Eq. (5) is accepted.

In Fig. 8, the SCFs extracted by the established formula are compared with the corresponding values obtained from FE analyses. From the value of R^2 ($R^2 = 0.945$), evaluating the equations based on the UK DoE (1980) standard, and Fig. 8, it can be seen that the derived formula is accurate enough to produce reliable results.

6. Conclusions

156 numerical models, verified against several available experimental tests, were produced to assess the stress concentration factors (SCFs) in the T-joints with ring under axial load. Through the analyses, the following conclusions were drawn:

- The present developed FE model is capable of modeling the SCFs in tubular T-joints reinforced with external ring subjected to axial load with enough accuracy.
- In T-joints reinforced with ring under axial load, against un-reinforced joint, the SCF at saddle point is significantly smaller than the SCF at crown point.
- The use of the ring can lead to the considerable decrement in the SCFs. Since, the ring enhances the stiffens of the joint intersection against ovalization and local bending of the chord.
- The increase of each the ring width or the ring thickness can result in a decrease in the SCFs. But, the effect of the ring width on the SCFs is slight.
- The rise of the τ, in fixed chord thickness, leads to the notable increase of the SCFs. However, the effect of the γ on the SCFs is slight.
- For determining the SCF in the reinforced T-joint at crown point, an empirical formula is proposed. A High determination factor (R^2 = 0.975), accepting the UK DoE (1980) criteria, and good match compared to corresponding values in a figure (Fig. 8) indicated that the proposed formula can be reliably applied for designing and stiffening tubular T-joints. Also, for determining the SCF in the joints at saddle point, the fixed value 1.5 is suggested. They can be widely used in the fatigue evaluation of offshore steel structures.

Acknowledgements

The authors gratefully acknowledge the useful comments of anonymous reviewers on the draft version of this paper.

References

Ahmadi, H. and Imani, H. (2022), “SCFs in offshore two-planar tubular TT-joints reinforced with internal ring stiffeners”, *Ocean Syst. Eng.*, **12**(1), 1-22. https://doi.org/10.12989/ose.2022.12.1.001.

American Welding Society (AWS), Structural Welding Code: AWS D 1.1. USA (2015).

Bao, S., Wang, W., Zhou, J., Qi, S. and Li, X. (2022), “Experimental study of hot spot stress for three-planar tubular Y-joint: I. Basic loads”, *Thin-Wall. Struct.*, **177**, 109418. https://doi.org/10.1016/j.tws.2022.109418.

Bomel Consulting Engineers. (1994), “Assessment of SCF equations using Shell/KSEPL finite element data”, C5970R02. 01 REV C.

Cai, Y.Q. and Shao, Y.B. (2011), “Stress concentration factor for circular tubular T-joints with collar plate reinforcement”, *J. Civ. Eng. Manage,* **2**(5).

Chang, E. and Dover, W.D. (1999), “Prediction of stress distributions along the intersection of tubular Y and T-joints”, *Int. J. Fatigue,* **21**(4), 361-381. https://doi.org/10.1016/S0142-1123(98)00083-8.

Elastic stress concentration factor tests on tubular steel joints – JISSP Wimpey Offshore. (1986).

Fung, T.C., Soh, C.K., Chan, T.K. and Erni (2002), “Stress concentration factors of doubler plate reinforced tubular T joints”, *J. Struct. Eng.*, **128**(11), 1399-1412. https://doi.org/10.1061/(ASCE)0733-9445(2002)128:11(1399).

Gho, W.M., Gao, F. and Yang, Y. (2006), “Strain and stress concentration of completely overlapped tubular CHS joints under basic loadings”, *J. Constr. Steel Res.*, **62**(7), 656-674. https://doi.org/10.1016/j.jcsr.2005.11.009.

Hectors, K. and De Waele, W. (2021), “Influence of weld geometry on stress concentration factor distributions in tubular joints”, *J. Constr. Steel Res.*, **176**, 106376. https://doi.org/10.1016/j.jcsr.2020.106376.

Hosseini, A.S., Bahaari, M.R. and Lesani, M. (2020), “Experimental and parametric studies of SCFs in FRP strengthened tubular T-joints under axially loaded brace”, *Eng. Struct.*, **213**, 110548.

https://doi.org/10.1016/j.engstruct.2020.110548

International Institute of Welding (IIW). (2008), Recommended Fatigue Design Procedure for Welded Hollow Section Joints-part 1: Recommendations, Part 2: Commentary. XV-1035–1099, Cedex, France.

Jiang, Y., Yuan, K. and Cui, H. (2018), "Prediction of stress concentration factor distribution for multi-planar tubular DT-joints under axial loads", *Mar. Struct.*, **61**, 434-451. https://doi.org/10.1016/j.marstruc.2018.06.017.

Kratzer, E. (1981), "Schwingfestigkeitsuntersunchungen as Rohrstruktukturelement-modellen von offshore plattformen Report BMFT-FB (M81)". (Cited by UK Health and Safety Executive. Prepared by Lloyd's Register of Shipping).

Liu, P.H., Chen, I.Y., Liu, X.Q., Su, C.K., Hsu, C.W., Dzeng, D.C. and Sung, Y.C. (2022), "Stress influence matrix on hot spot stress analysis for welded tubular joint in offshore jacket structure", *Ocean Eng.*, **251**, 111103. https://doi.org/10.1016/j.oceaneng.2022.111103.

Melek, P.G., Gaawan, S. and Osman, A. (2020), "Strengthening steel CHS X-joints subject to compression by outer ring stiffeners", *Int. J. Steel Struct.*, **20**, 1115-1134. https://link.springer.com/article/10.1007/s13296-020-00346-0.

Mohamed, H.S., Zhang, L., Shao, Y.B., Yang, X.S., Shaheen, M.A. and Suleiman, M.F. (2022), "Stress concentration factors of CFRP-reinforced tubular K-joints via zero point structural stress approach", *Mar. Struct.*, **84**, 103239. https://doi.org/10.1016/j.marstruc.2022.103239.

Musa, I.A., Mashiri, F.R., Zhu, X. and Tong, L. (2018), "Experimental stress concentration factor in concrete-filled steel tubular T-joints", *J. Constr. Steel Res.*, **150**, 442-451. https://doi.org/10.1016/j.jcsr.2018.09.001.

Myers, P.T., Brennan, F.P. and Dover, W.D. (2001), "The effect of rack/rib plate on the stress concentration factors in jack-up chords", *Mar. Struct.*, **14**(4-5), 485-505. https://doi.org/10.1016/S0951-8339(00)00051-4.

N'diaye, A., Hariri, S., Pluvinage, G. and Azari, Z. (2009), "Stress concentration factor analysis for welded, notched tubular T-joints under combined axial, bending and dynamic loading", *Int. J. Fatigue*, **31**(2), 367-374. https://doi.org/10.1016/j.ijfatigue.2008.07.014.

Nassiraei, H. (2020), "Local joint flexibility of CHS T/Y-connections strengthened with collar plate under in-plane bending load: parametric study of geometrical effects and design formulation", *Ocean Eng.*, **202**, 107054. https://doi.org/10.1016/j.oceaneng.2020.107054.

Nassiraei, H. and Rezadoost, P. (2022), "Probabilistic analysis of the SCFs in tubular T/Y-joints reinforced with FRP under axial, in-plane bending, and out-of-plane bending loads", *Structures*, **35**, 1078-1097. https://doi.org/10.1016/j.istruc.2021.06.029.

Nassiraei, H. (2022), "Geometrical effects on the LJF of tubular T/Y-joints with doubler plate in offshore wind turbines", *Ships Offshore Struct.*, **17**(3), 481-491. https://doi.org/10.1080/17445302.2020.1835051.

Nassiraei, H. and Rezadoost, P. (2020), "Stress concentration factors in tubular T/Y-joints strengthened with FRP subjected to compressive load in offshore structures", *Int. J. Fatigue*, **140**, 105719. https://doi.org/10.1016/j.ijfatigue.2020.105719.

Nassiraei, H. and Rezadoost, P. (2021a), "Stress concentration factors in tubular T/Y-connections reinforced with FRP under in-plane bending load", *Mar. Struct.*, **76**, 102871. https://doi.org/10.1016/j.marstruc.2020.102871.

Nassiraei, H. and Rezadoost, P. (2021b), "Local joint flexibility of tubular X-joints stiffened with external ring or external plates", *Mar. Struct.*, 80, 103085. https://doi.org/10.1016/j.marstruc.2021.103085.

Pan, Z., Wu, G., Si, F., Shang, J., Zhou, H., Li, Q. and Zhou, T. (2022), "Parametric study on SCF distribution along the weld toe of internally ring-stiffened two-planar tubular KK joints under axial loading", *Ocean Eng.*, **248**, 110826. https://doi.org/10.1016/j.oceaneng.2022.110826.

Recommended Practice for Planning, Designing and Constructing FIxed Offshore Platforms: Working Stress Design: RP2A-WSD. (2015), twenty-first ed, US, Washington, DC.

Shao, Y.B. (2007), "Geometrical effect on the stress distribution along weld toe for tubular T-and K-joints under axial loading", *J. Constr. Steel Res.*, **63**(10), 1351-1360. https://doi.org/10.1016/j.jcsr.2006.12.005.

Shen, W. and Choo, Y.S. (2012), "Stress intensity factor for a tubular T-joint with grouted chord", *Eng. Struct.*, **35**, 37-47. https://doi.org/10.1016/j.engstruct.2011.10.014.

Soh, A.K. and Soh, C.K. (1995), "Stress analysis of axially loaded T tubular joints reinforced with doubler plates", *Comput. Struct.*, **55** (1), 141-149. https://doi.org/10.1016/0045-7949(94)00412-V.

Swensson, K.D. and Yura, J.A. (1986), "Stress Concentration Factors in Double-Tee Tubular Joints PMFSEL Report No".

Tong, L.W., Chen, K.P., Xu, G.W. and Zhao, X.L. (2019), "Formulae for hot-spot stress concentration factors of concrete-filled CHS T-joints based on experiments and FE analysis", *Thin-Wall. Struct.*, **136**, 113-128. https://doi.org/10.1016/j.tws.2018.12.013.

UK Department of Energy (DoE). (1983), "Background notes to the fatigue guidance of offshore tubular joints".

UKOSRP I final report UKOSRPI I, (1980).

Wordsworth, A.C. (1979), "Stress concentration at tubular Y and oblique X joints Contract No. 62/04150343".

Xu, F., Chen, J., and Jin, W. L. (2015), "Experimental investigation of SCF distribution for thin-walled concrete-filled CHS joints under axial tension loading", *Thin-Wall. Struct.*, **93**, 149-157. https://doi.org/10.1016/j.tws.2015.03.019.

Xu, X., Shao, Y., Gao, X. and Mohamed, H.S. (2022), "Stress concentration factor (SCF) of CHS gap TT-joints reinforced with CFRP", *Ocean Eng.*, **247**, 110722. https://doi.org/10.1016/j.oceaneng.2022.110722.

Yang, K., Zhu, L., Bai, Y., Sun, H. and Wang, M. (2018), "Strength of external-ring-stiffened tubular X-joints subjected to brace axial compressive loading", *Thin-Wall. Struct.*, **133**, 17-26. https://doi.org/10.1016/j.tws.2018.09.030.

Zhao, L., Zhu, L., Sun, H., Yang, L. and Chen, X. (2020), "Experimental and numerical investigation of axial tensile strength of CHS X-joints reinforced with external stiffening rings", *Int. J. Steel Struct.*, **20**(3), 1003-1013. https://doi.org/10.1007/s13296-020-00337-1.

Zhao, X.L., Herion, S., Packer, J.A., Puthli, R., Sedlacek, G., Wardenier, J. and Yeomans, N. (2000), "Design guide for circular and rectangular hollow section joints under fatigue loading. CIDECT, TUV".

Zhu, L., Yang, K., Bai, Y., Sun, H. and Wang, M. (2017), "Capacity of steel CHS X-joints strengthened with external stiffening rings in compression", *Thin-Wall. Struct.*, **115**, 110-118. https://doi.org/10.1016/j.tws.2017.02.013.

AK